| | | |
|---|---|---|
| ESRF | **Experiment title:**<br>Electronic and structural changes of Mn in $Nd_{0.5}Sr_{0.5}MnO_3$ crossing the magnetoresistive and charge-ordering transitions by high resolution XAS/XES. | **Experiment number**:<br>HC-1997 |
| **Beamline**:<br>ID26 | **Date of experiment**:<br>from: 27/02/2015 to: 06/03/2015 | **Date of report**:<br>31-08-2015 |
| **Shifts:**<br>18 | **Local contact(s)**:<br>S. Lafuerza | *Received at ESRF:* |

**Names and affiliations of applicants** (* indicates experimentalists):

Sara Lafuerza[1*], Joaquín García[2*], Javier Blasco[2*], and Gloria Subías[2*]

[1] ESRF, 71 rue Jules Horowitz CS 40220, FR-38043 Grenoble Cedex (France)
[2] Instituto de Ciencia de Materiales de Aragón, Universidad de Zaragoza – CSIC, C/ Pedro Cerbuna 12 ES - 50009 Zaragoza (Spain)

## Report:

Mixed-valence $Nd_{0.5}Sr_{0.5}MnO_3$ is a very fascinating compound as it shows several phases as a function of temperature: (i) T > 230 K: paramagnetic insulator, (ii) 170 K ≤ T ≤ 230 K: ferromagnetic metal and (iii) T < 170 K: antiferromagnetic, charge ordered state. The main objective of this study was then to probe the changes in the electronic structure as a function of temperature across the different phases. Accordingly, a thorough investigation was carried out by means of XAS/XES/RIXS for both the Mn Kβ and Kα emission lines regions. Besides, the reference compounds $NdMnO_3$ ($Mn^{3+}$), $CaMnO_3$ ($Mn^{4+}$) and $SrMnO_3$ ($Mn^{4+}$) were measured for the sake of comparison. $CaMnO_3$ and $SrMnO_3$ only undergo antiferromagnetic transitions at $T_N$ about 110 and 230-260 K respectively.

The incident energy was tuned through the Mn K-edge by means of a pair of cryogenically cooled Si(311) monochromator crystals. The measurements can be divided into two different sets according to the Mn Kβ and Kα emission lines parts. The inelastically scattered photons were analyzed using sets of four spherically bent Ge(440) and Ge(333) crystals for the Mn Kβ and Kα lines respectively. The crystals were arranged with samples and photon detector (Avalanche Photo Diode) in a vertical Rowland geometry (R ≈ 1 m). We used masks in the crystals to improve resolution which was about 0.7 and 0.4 eV for the Mn Kβ and Kα lines respectively, as deduced from the full width half maximum of the elastic peaks. HERFD-XANES across the Mn K-edge (6.539 eV) were recorded at the maximum of the Mn $K\beta_{1,3}$, Kβ' and $K\alpha_1$ lines for each compound. In the case of the Mn $K\alpha_1$ line and only for $Nd_{0.5}Sr_{0.5}MnO_3$, also EXAFS spectra were collected. Non-resonant Mn Kβ core-to-core (CTC), valence-to-core (VTC) and Kα XES spectra were measured at incident energy ($E_i$) 6700 eV. Finally, 1*s*2*p* RIXS maps as well as RIXS data in the region of the CTC and VTC lines were collected in selected cases. The measurements were carried out on pure pellets after finding no difference in the spectra as compared with 5 – 10% in mass diluted pellets. A continuous He-flow cryostat was used to carry out temperature-dependent measurements.

In general, it can be said from all the abovementioned measurements that the main changes in the electronic structure are seen between the different compounds rather than in $Nd_{0.5}Sr_{0.5}MnO_3$ as a function of temperature, despite the different macroscopic properties in each of the phases. Regarding the emission spectra, $Nd_{0.5}Sr_{0.5}MnO_3$ shows a closer behaviour to $NdMnO_3$ ($Mn^{3+}$) than to $SrMnO_3$/$CaMnO_3$ ($Mn^{4+}$) as follows from the position in energy of the $K\beta_{1,3}$, $K\beta_{2,5}$ and $K\alpha_1$ lines. Figure 1 shows as example the Mn Kβ CTC XES spectra at room temperature and the spin (S) values derived from these data as a function of temperature using the so-called integrated absolute difference (IAD) method. We have converted the IAD

values into S by using the linear relationship IAD-S obtained from the data of the two binary oxides $MnO_2$ (S = 3/2) and $Mn_2O_3$ (S = 2). We have also found that the weight needed in the spectra of $NdMnO_3$ and $SrMnO_3$ to reproduce the $Nd_{0.5}Sr_{0.5}MnO_3$ spectrum is not simply equal to the doping concentration but much closer to 0.7 $NdMnO_3$ + 0.3 $SrMnO_3$ (not shown).

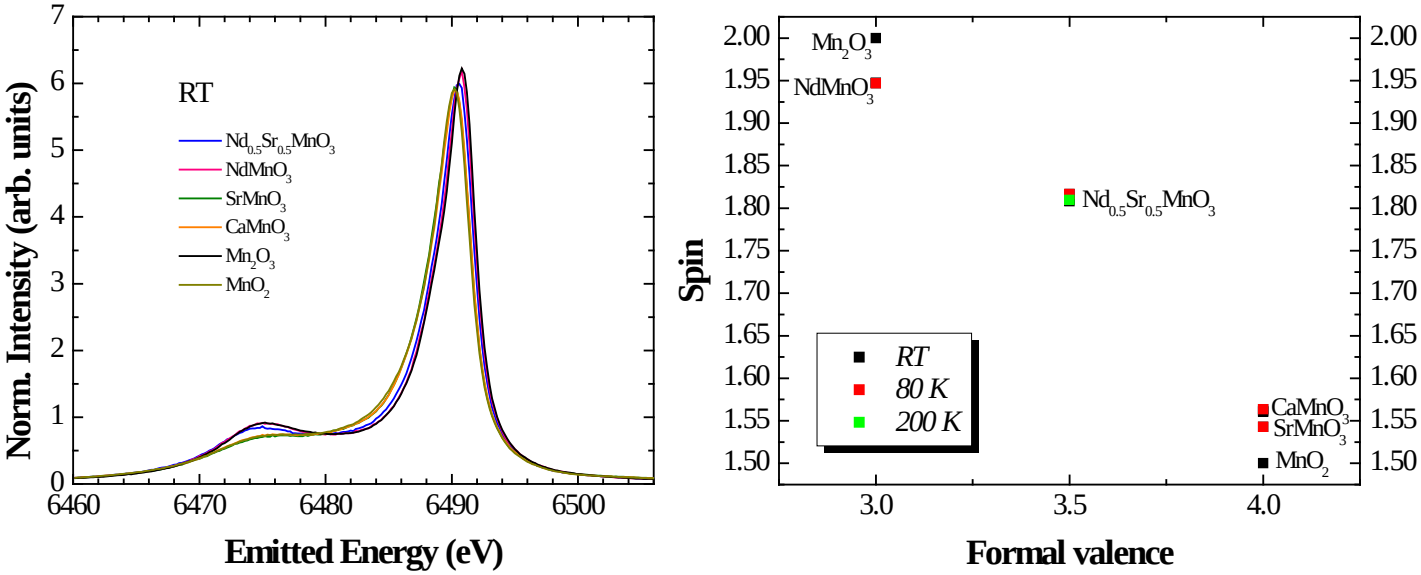


Figure 1. (Left) Mn $K\beta_{1,3}$ and $K\beta'$ CTC XES spectra of the different compounds at RT. (Right) Spin values derived from the IAD analysis plotted versus formal valence.

On the other hand, the HERFD-XANES at the Mn K-edge show a rich pre-peak structure that it is best resolved in the measurements collected at the maximum of the $K\alpha_1$ line. The difference signal obtained by substracting the data at 292 K from all the data files (at different temperatures upon cooling down) has been evaluated to better elucidate the possible changes. Figure 2 shows the results for the $Nd_{0.5}Sr_{0.5}MnO_3$ compound. In the preedge region, a temperature variation of the $A_1$ and $A_2$ peaks is clearly visible: below 240 K, the $A_1$ difference peak increases, with most of the change occurring over a 80 K-range just below entering the ferromagnetic-metal phase. Upon cooling down into the antiferromagnetic-charge ordered phase, the change of the $A_1$ peak with T is inverted – it decreases instead of continuously increasing. Besides, the HERFD-EXAFS at the $K\alpha_1$ line have been combined with the simultaneously measured TFY-EXAFS to get rid of the self-absorption from Nd and allow for a sufficiently long range in *k* for quantitative analysis in the case of the $Nd_{0.5}Sr_{0.5}MnO_3$. We note that the EXAFS spectra suffer from Nd self-absorption ($L_2$-edge at 6.722 keV and $L_3$-edge at 6.208 keV) which appears as dips and peaks in the HERFD and TFY data respectively. The EXAFS analysis points out that the local distortion of the $MnO_6$ octahedron present in the paramagnetic-semiconducting phase at room temperature decreases upon cooling into the ferromagnetic-metallic phase although it does not collapse as occurs in the magnetoresistive samples but it remains slightly distorted in the antiferromagnetic-charge ordered phase.

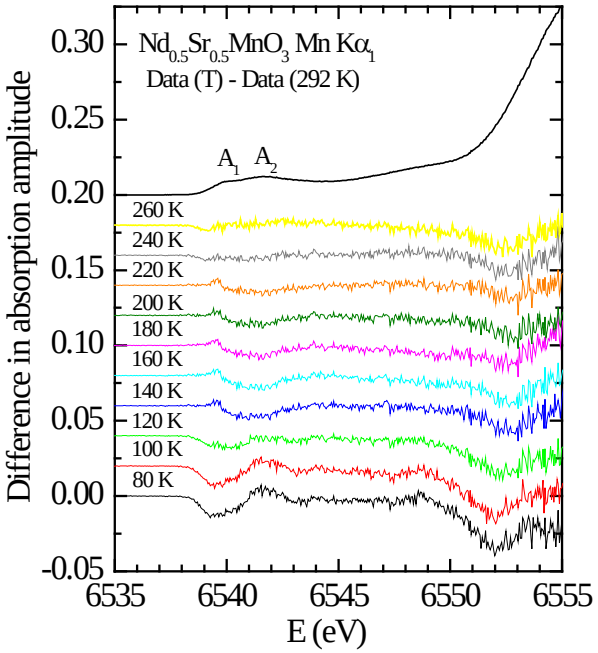


Figure 2. Difference HERFD-XANES data measured at the $K\alpha_1$ line for $Nd_{0.5}Sr_{0.5}MnO_3$ between 292 K and each T.

Finally, the analysis of the spin-selective HERFD-XANES at the maximum of $K\beta_{1,3}$ and $K\beta'$ as well as of the different RIXS maps in which the pre-peak structure was studied scanning also the emitted energy in the range of the Mn Kβ (main lines and satellites) and Kα lines, is currently in progress.